Chinese Chemical Letters 31 (2020) 1402–1405

Contents lists available at ScienceDirect

Chinese Chemical Letters

journal homepage: www.elsevier.com/locate/cclet

Communication

# Insights into bishemicyanines with long emission wavelengths and high sensitivity in viscous environments

Jianfang Cao[a,b], Wen Sun[a], Jiangli Fan[a,*]

[a] State Key Laboratory of Fine Chemicals, Dalian University of Technology, Dalian 116024, China
[b] School of Chemical and Environmental Engineering, Liaoning University of Technology, Jinzhou 121001, China

ARTICLE INFO

*Article history:*
Received 3 September 2019
Received in revised form 8 October 2019
Accepted 9 October 2019
Available online 14 October 2019

*Keywords:*
Bishemicyanine dyes
Long emission wavelength
Low background quantum yield
Rotating energy barrier
Density functional calculations

ABSTRACT

A systematic spectral analysis was presented for bishemicyanine dyes (Hsd and D2) and monohemicyanine dyes (Hs and DSMI). The bishemicyanine dyes displayed long emission wavelengths, large Stokes shifts, low background quantum yields in aqueous solutions and high sensitivity in viscous environments. Better understanding of the structure-property relationships could benefit the design of improved dyes. Computational studies on these dyes revealed the three conjugated forms of bishemicyanines are in equilibrium due to two positive charges and a branched bulk substituent. Bishemicyanines possessed obviously lower rotating energy barrier of C—C bond rotation compared to the monohemicyanine dyes. Moreover, the synergetic effects of the rotation about the $\phi_4$ bond, $\phi_5$ bond and $\phi_7$ bond of the bishemicyanines (Hsd and D2) lead to lower fluorescence quantum yields in a free state and larger fluorescence quantum yield enhancements in viscous environment compared to that of monohemicyanine dyes (Hs and DSMI). The results demonstrate a foundation for interpretation of the behavior of the dyes, thus providing guidelines for future of new bishemicyanine fluorophores with specific applications.



Hemicyanines are widely used in biotechnology due to good biocompatibility and low toxicity to biosamples [1–5]. They possess relatively low fluorescence quantum yields (<1%) in an aqueous solution [6–9]. However, their fluorescence lifetime and quantum yields are known to realize the fluorescence response to the restricted intracellular nucleic acid micro-environment and viscous environment due to the inhibition of the rotation for hemicyanines [10–15]. To enrich hemicyanine scaffolds with tunable emission wavelengths and provide a high sensitivity in the intracellular microenvironment, numerous attempts have been made [16–25]. Wong reported V-carbazole exhibited high sensitivity and efficiency for double-stranded DNA (dsDNA) because of the selective binding interaction with the AT-rich regions [26]. Our group introduced a pyridiumvinyl group into the aniline ring of DSMI (*trans*-4-[4-(dimethylamino)styryl]-1-methylpyridinium iodide) to form bishemicyanine dye D2 (2,4-bis[(*E*)-*N*-methyl-4-pyridinyl ethenyl]-1-dimethylamino benzene diiodide). The emission spectrum of dye D2 reaches the red light region, and the dye D2 has a large Stokes shift [27]. In addition, we further synthesized a novel bishemicyanine dye Hsd (2,4-bis[(*E*)-*N*-methyl-2-benzothiazolium vinyl]-1-dimethylaminobenzene diiodide) by introducing benzothiazoliumyl vinyl moiety into ethenyl-3-methylbenzothiazolium iodide, which was found to be a potential RNA fluorescent probe in NIR region for HeLa cell staining [28]. We found bishemicyanines (Hsd and D2) display unprecedented red and near infrared (NIR) maximum emission wavelengths, large Stokes shifts and extremely low background fluorescence quantum yields (<0.001) in an aqueous solution, compared to those of monohemicyanines (Hs and DSMI), which overcomes the limitations of the self-aggregation effect encountered by conventional cyanine dyes. Until recently, the in-depth mechanism of the fluorogenic behavior for bishemicyanines is still unknown.

In the current work, we systematically studied the spectral properties, fluorescence quantum yields, viscosity response of Hs, Hsd, DSMI and D2 (Scheme 1). Theoretical simulations are recognized as a powerful tool to study the photophysical properties of fluorophores and the mechanisms for fluorogenic behavior. Therefore, we further analyzed molecular geometries, the frontier molecular orbitals and the branched bulk substituent effect on the rotation of polymethine-chain of the dyes by theoretical calculation. Long wavelengths and large Stokes shifts are well explained by molecular geometries and molecular orbitals. A detailed study of the potential energy curves of the

* Corresponding author.
*E-mail address:* fanjl@dlut.edu.cn (J. Fan).

https://doi.org/10.1016/j.cclet.2019.10.006

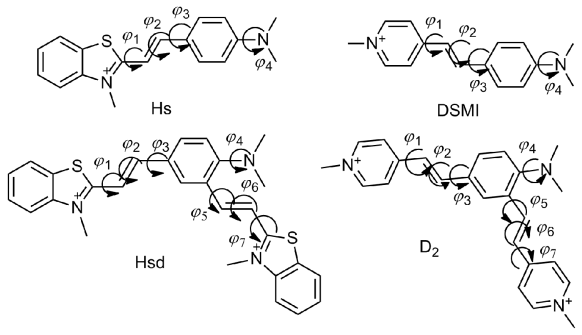


**Scheme 1.** Chemical structures of Hs, Hsd, DSMI and D2 dyes.

different twisting angles for the four dyes provided a reasonable explanation that bishemicyanines (Hsd and D2) have lower fluorescence quantum yields in a free state and larger fluorescence quantum yield enhancement in a viscous environment. We hope our work would be helpful to study the relationship between molecular structures and required properties of other fluorescent dyes.

Hs, Hsd, DSMI and D2 were prepared according to our previous work [27,28]. Fluorescence spectra were obtained with a Felix and Time-Masters PTI-C-700 system. Visible absorption spectra were determined using an Agilent HP-8453 spectrophotometer.

The molecular geometries (the atomic standard orientations after geometry optimization of ground state and excited state have been given in Supporting information) were investigated using density functional theory (DFT) and time-dependent density functional theory (TDDFT) calculations. A test of functionals was performed for photochemical properties of the Hs and Hsd (Tables S1 and S2 in Supporting information). The $\tau$-dependent member of the HCTH family (tHCTHhyb functional) was proven to be a better choice in accordance with the experimental results [29], thus used in both the DFT and TD-DFT. The triple-$\zeta$ valence quality with one set of polarization functions (TZVP) was chosen as the basis set throughout, which is appropriate for such organic compound [30,31]. Moreover, electronic excitation energies of low-lying electronically excited states were also computed by the TDDFT method. A continuum solution model, COSMO (conductor-like screening model) was used for the consideration of solvent effects in aqueous solution [32]. Harmonic vibrational frequency calculations were made by using tHCTHhyb/TZVP to confirm the energy minima for all the structures. In addition, the $S_0$ and $S_1$ potential energy curves were qualitatively scanned by constrained optimizations, keeping the dihedral angels fixed at a series of values. All calculations on electronic structures were carried out using the Gaussian 09 program suite.

To better understand the photophysical properties and fluorescence response to solvent viscosity of bishemicyanines and a monohemicyanine, we further collected absorption and fluorescence spectra of Hs, Hsd, DSMI and D2 in different solvents and proportions of water-glycerol systems. Monohemicyanine Hs possessed only one absorption and emission peak ($\lambda_{abs}/\lambda_{em}$ = 512/580 nm) in aqueous solution (Fig. 1 and Fig. S1 in Supporting information). However, bishemicyanine Hsd displayed two absorption peaks at 458 nm and 363 nm (Fig. S1) and two emission peaks at 620 nm and 580 nm in an aqueous solution (Fig. 1). Compared with Hs, the absorption peak of Hsd blue shifted from 512 nm to 458 nm and 363 nm; emission peak red shifted from 580 nm to 620 nm. The Stokes shift of the dye was enlarged from less than 68 nm to more than 224 nm in an aqueous solution. Similarly, compared with DSMI, the absorption peak of D2 blue shifted from *ca.* 450 nm to *ca.* 393 nm and 345 nm (Fig. S2 in Supporting information); emission peak red shifted from *ca.* 610 nm to *ca.* 615 nm (Fig. S3 in Supporting information). The Stokes shift of the dye was enlarged from less than 160 nm to more than 222 nm in water. It should also be pointed out that bishemicyanines displayed long emission wavelengths and large Stokes shifts, which possess better tissue penetration, lower phototoxicity and less photodamage to biological samples. In nonviscous solvents, the polar solvents demonstrated little effect on fluorescence enhancements for these dyes (Fig. 1 and Fig. S3), which is crucial for a molecular rotor to sense environmental viscosity.

The optical responses to the viscosity of Hs, Hsd, DSMI and D2 were first evaluated. When glycerol was gradually increased in water, the viscosity of the solutions increased from 0.9 cp (water) to *ca.* 940 cp (99% glycerol) and paralleling fluorescence enhancements of the four dyes increased continuously (Fig. 1 and Fig. S4 in Supporting information). The fluorescence quantum yield of the Hsd was 0.0209 in the solution of 99% glycerol and 0.0002 in the solution of pure water, approximately 85-fold enhancement (Table 1). There was about 33-fold increase in the fluorescence quantum yield for Hs; from 0.0022 in the solution of pure water to 0.0744 in the solution of 99% glycerol. Similarly, the DSMI exhibited *ca.* 51-fold increase in fluorescence quantum yield when the ratio of glycerol was increased from 0% to 99% and D2 displayed *ca.* 86-fold enhancement under identical conditions system. For the same viscosity, the fluorescence enhancement of bishemicyanine is much stronger than monohemicyanine. Notably, monohemicyanine (Hs and DSMI) exhibited low fluorescence quantum yield in water whereas bishemicyanines (Hsd and D2) typically showed *ca.*10-fold decrease, with respect to that of monohemicyanine. Dyes with a low quantum yield corresponding to a low non-signal background provides highly sensitive viscosity detection when the fluorescence enhancement is in the same target range [33,34]. In order to better interpret such experimental findings, further theoretical calculation has been performed concerning the geometry, spectra, molecular orbitals and potential energy curves.

The energy separations for the absorption $\Delta E_{abs}$(nm), emission $\Delta E_{em}$(nm) and corresponding oscillator strengths of the low-lying electronically excited states for Hs, Hsd, DSMI and D2 are presented in Table S3 (Supporting information). The calculated absorption and emission peaks of Hs 492 nm ($S_0 \rightarrow S_1$, HOMO→LUMO) and

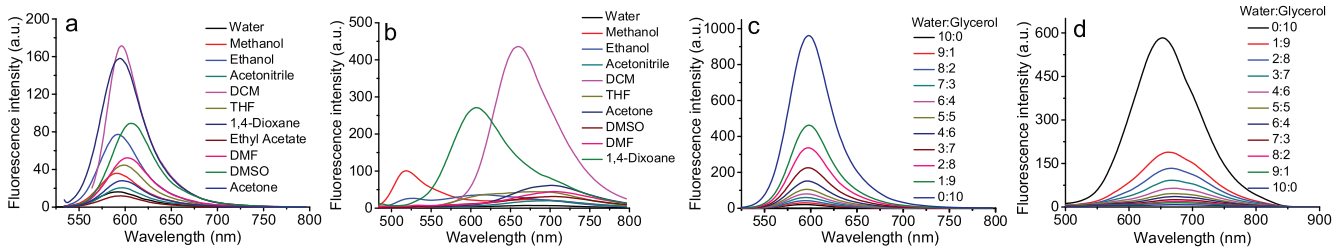


**Fig. 1.** The emission spectra of Hs excited at 509 nm (a) and Hsd excited at 458 nm (b) in different solvents. Fluorescence changes of Hs excited at 533 nm (c) and Hsd excited at 477 nm (d) in water-glycerol systems with different proportional glycerol.

**Table 1**
Fluorescence quantum yields ($\Phi_f$) recorded in water and 99% glycerol.

| Dye | $\lambda_{abs}$ (nm) | $\lambda_{em}$ (nm) | Stokes shift (nm) | $\Phi_f$ (water) | $\Phi_f$ (99% glycerol) |
|---|---|---|---|---|---|
| Hs | 512 | 580 | 68 | $2.22 \times 10^{-3}$ | $7.45 \times 10^{-2}$ (33-fold) |
| Hsd | 458 (363) | 682 (580) | 224 | $2.46 \times 10^{-4}$ | $2.09 \times 10^{-2}$ (85-fold) |
| DSMI | 450 | 610 | 160 | $2.00 \times 10^{-3}$ | $9.45 \times 10^{-2}$ (51-fold) |
| D2 | 393 (345) | 615 (530) | 222 | $5.05 \times 10^{-4}$ | $4.37 \times 10^{-2}$ (86-fold) |

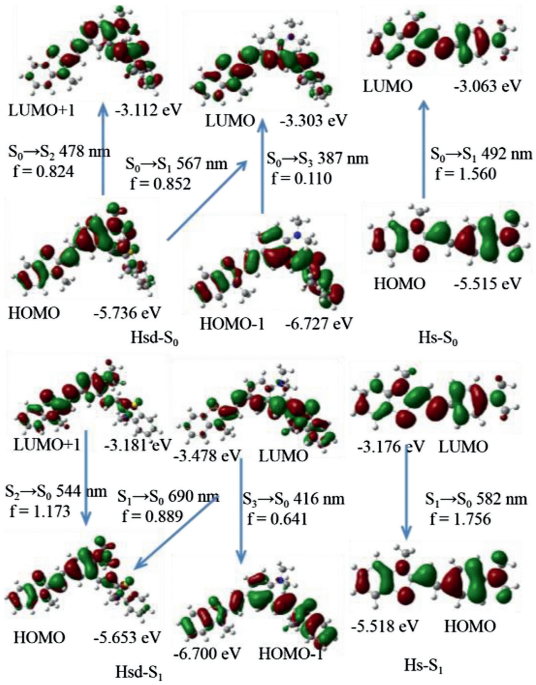


**Fig. 2.** The frontier molecular orbitals of the ground-state geometry $S_0$ and relaxed excited state $S_1$ for the Hs and Hsd.

582 nm ($S_1 \rightarrow S_0$, LUMO→HOMO) respectively in Fig. 2 were consistent with the experimental data. Hsd showed three absorption peaks in Fig. 2: 478 nm ($S_0 \rightarrow S_2$, HOMO→LUMO+1) due to conjugate field between $N(CH_3)_2$ and the *p*-substituted benzothiazolium vinyl moiety which is similar to Hs. The other absorption peak at 387 nm ($S_0 \rightarrow S_3$, HOMO-1→LUMO) can be assigned to the part from $N(CH_3)_2$ to the *o*-substituted benzothiazolium vinyl moiety which forms a smaller conjugate system than Hs. The absorption maxima for Hsd at 567 nm ($S_0 \rightarrow S_1$, HOMO→LUMO) arises from the conjugate field between *p*-substituted and the *o*-substituted benzothiazolium vinyl moiety, similar to that of heptamethine cyanine dye (Cy7). The calculated excited state ($S_1$) emission peak at 690 nm is in good agreement with emission band at 682 nm observed in an aqueous solution. The second excited state emission peak 544 nm of Hsd is in good agreement with emission band at 580 nm observed in an aqueous solution. The short-wavelength emission at 416 nm originates only from the $S_3$ state, which is not easy to appear in an aqueous solution due to relatively small transition probability. The orbital transitions of DSMI (Fig. S6 in Supporting information) are similar to those of Hs. The orbital transitions of D2 (Fig. S7 in Supporting information) are also similar to those of Hsd. Moreover, the three conjugated forms of bishemicyanines (Hsd and D2) are in equilibrium due to the rotational motion of the dyes skeletons in aqueous solution. A thorough elucidation of the calculated absorption and emission energies of the four dyes has been carried out to support our experimental results. The dyes (Hsd and D2) transferred from ground state to the vertical excited state ($S_2$ state and $S_3$ state) by excitation. The vertical excited state changes their configuration to the first excited state $S_1$, and then returns to the ground state through emitting long wavelength fluorescence. There are obvious intramolecular charge transfers from the ground state to the excited state for the two dyes (Hsd and D2). The changes of geometry configurations (Fig. S5 and Table S4 in Supporting information) and an obvious intramolecular charge transfer are responsible for the large Stokes shift of the two dyes (Hsd and D2).

The potential energy curves of the rotating C—C bond of the four dyes were investigated. The height of the energy barrier in the excited state strongly depends on the position of the rotating C—C bond [35,36]. The lowest energy path for the nonradiative internal conversion process of the Hs is associated with the rotation about the $\phi_3$ bond close to the phenyl moiety of the polymethine chain, with a low energy barrier of 2.605 kcal/mol (Fig. 3, Fig. S8 and Table S5 in Supporting information). For Hsd, the potential energy curves suggest that the rotation about the $\phi_4$ bond, $\phi_5$ bond and $\phi_7$ bond are very easy, since they have low barrier to rotation in the $S_1$ state (Fig. 3, Fig. S9 and Table S6 in Supporting information). The rotations of $\phi_1$ bond, $\phi_2$ bond, $\phi_3$ bond and $\phi_6$ bond are not advantageous, since they have higher energy barriers to rotation in the $S_1$ state. Compared with Hs, Hsd with the relatively lower energy barrier is a facilitated efficient nonradiative internal conversion. The synergetic effect of the rotation about the $\phi_4$ bond, $\phi_5$ bond and $\phi_7$ bond of the Hsd leads to lower background fluorescence quantum yield and larger fluorescence quantum yield enhancement in viscosity compared to that of monocyanine Hs. The potential energy curves of DSMI (Table S7 and Fig. S10 in Supporting information) are similar to those of Hs and that of D2 (Table S8 and Fig. S11 in Supporting information) also similar to those of Hsd. The branched bulk substituent plays a major role in determining background fluorescence quantum yield and environmental sensitivity.

In conclusion, bishemicyanine dyes (Hsd and D2) showed unique spectroscopic characteristic such as very low fluorescence quantum yields (0.0002–0.0005) in non-viscous solvents and large Stokes shifts (>200 nm). We have clarified the introduction of two positive charges and a branched bulk substituent of the monohemicyanine dyes leads to significant low background fluorescence quantum yields. For Hsd

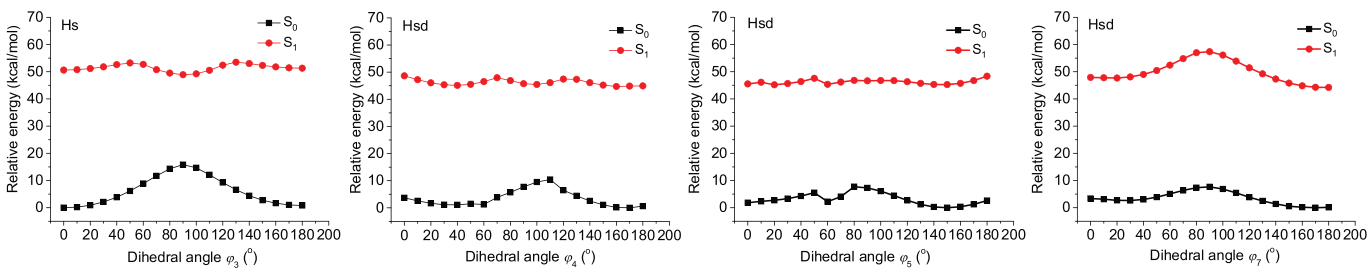


**Fig. 3.** Energy levels of the $S_0$ (black) and $S_1$ (red) states of Hs rotation along with dihedral angle $\phi_3$ and Hsd rotation along with dihedral angle $\phi_4$, $\phi_5$ and $\phi_7$.

and D2, the rotation about the $\phi_4$ bond, $\phi_5$ bond and $\phi_7$ bond are very easy in the $S_1$ state, resulting in efficient non-radiative internal conversion and significant environmental sensitivity. These results might provide a foundation for interpretation of the behavior of these dyes and are useful for future design of new bishemicyanine fluorophores thus could be employed in highly sensitive environmental detection and biomedical imaging applications.

## Declaration of competing interest

The authors declare that they have no known competing financial interests or personal relationships that could have appeared to influence the work reported in this paper.

## Acknowledgments

This work was financially supported by the National Natural Science Foundation of China (No. 21606118) and the State Key Laboratory of Fine Chemicals (No. KF1614).

## Appendix A. Supplementary data

Supplementary material related to this article can be found, in the online version, at doi:https://doi.org/10.1016/j.cclet.2019.10.006.

## References

[1] Y.V. Suseela, N. Narayanaswamy, S. Pratihar, T. Govindaraju, Chem. Soc. Rev. 47 (2018) 1098–1131.
[2] S. Samanta, S. Halder, G. Das, Anal. Chem. 90 (2018) 7561–7568.
[3] T. Zhu, J. Du, W. Cao, J. Fan, X. Peng, Ind. Eng. Chem. Res. 55 (2016) 527–533.
[4] J. Cui, Y. Yao, C. Chen, et al., Chin. Chem. Lett. 30 (2019) 1071–1074.
[5] W. Sun, S. Guo, C. Hu, J. Fan, X. Peng, Chem. Rev. 116 (2016) 7768–7817.
[6] Y. Huang, T. Cheng, F. Li, et al., J. Phys. Chem. B 106 (2002) 10041–10050.
[7] T. Shim, M.H. Lee, D. Kim, H.S. Kim, K.B. Yoon, J. Phys. Chem. B 113 (2009) 966–969.
[8] K. Bi, R. Tan, R. Hao, et al., Chin. Chem. Lett. 30 (2019) 545–548.
[9] Z. Pillai, P.K. Sudeep, K.G. Thomas, Res. Chem. Intermed. 29 (2003) 293–305.
[10] C.Q. Zhu, S.J. Zhuo, H. Zheng, et al., Analyst 129 (2004) 254–258.
[11] L. Guo, M.S. Chan, D. Xu, et al., ACS Chem. Biol. 10 (2015) 1171–1175.
[12] K. Zhou, M. Ren, B. Deng, W. Lin, New J. Chem. 41 (2017) 11507–11511.
[13] G. Hungerford, A. Allison, D. McLoskey, et al., J. Phys. Chem. B 113 (2009) 12067–12074.
[14] Y. Shiraishi, T. Inoue, T. Hirai, Langmuir 26 (2010) 17505–17512.
[15] B. Wandelt, P. Cywinski, G.D. Darling, B.R. Stranix, Biosens. Bioelectron. 20 (2005) 1728–1736.
[16] J.T. Miao, C. Fan, R. Sun, Y.J. Xu, J.F. Ge, J. Mater. Chem. B 2 (2014) 7065–7072.
[17] L. Yuan, W. Lin, Y. Yang, H. Chen, J. Am. Chem. Soc. 134 (2012) 1200–1211.
[18] D. Wu, Y. Shen, J. Chen, et al., Chin. Chem. Lett. 28 (2017) 1979–1982.
[19] F. Liu, T. Wu, J. Cao, et al., Chem.-Eur. J. 19 (2013) 1548–1553.
[20] S.I. Reja, I.A. Khan, V. Bhalla, M. Kumar, Chem. Commun. (Camb.) 52 (2016) 1182–1185.
[21] L. Yu, Q. Yang, Y. Tang, Chin. Chem. Lett. 30 (2019) 694–697.
[22] Y. Jin, X. Tian, L. Jin, et al., Anal. Chem. 90 (2018) 3276–3283.
[23] A.J. Chung, P.S. Deore, S. Al-Abdul-Wahid, et al., J. Org. Chem. 84 (2019) 2261–2268.
[24] Z.Z. Gao, J. Kan, Z. Tao, B. Bian, X. Xiao, New J. Chem. 42 (2018) 15420–15426.
[25] X. Lv, J. Liu, Y. Liu, et al., Chem. Commun. (Camb.) 47 (2011) 12843–12845.
[26] X.J. Feng, P.L. Wu, F. Bolze, et al., Org. Lett. 12 (2010) 2194–2197.
[27] S. Sun, Y. Yuan, Z. Li, et al., New J. Chem. 38 (2014) 3600–3605.
[28] Z. Li, S. Sun, Z. Yang, et al., Biomaterials 34 (2013) 6473–6481.
[29] A.D. Boese, N.C. Handy, J. Chem. Phys. 116 (2002) 9559–9569.
[30] J.F. Cao, C. Hu, W. Sun, et al., RSC Adv. 4 (2014) 13385–13394.
[31] O. Treutler, R. Ahlrichs, J. Chem. Phys. 102 (1995) 346–354.
[32] J.F. Cao, C. Hu, F. Liu, et al., ChemPhysChem 14 (2013) 1601–1608.
[33] M.K. Kuimova, G. Yahioglu, J.A. Levitt, K. Suhling, J. Am. Chem. Soc. 130 (2008) 6672–6673.
[34] J.F. Cao, T. Wu, C. Hu, et al., Phys. Chem. Chem. Phys. 14 (2012) 13702–13708.
[35] A.C. Benniston, A. Harriman, V.L. Whittle, M. Zelzer, Eur. J. Org. Chem. 2010 (2010) 523–530.
[36] G.L. Silva, V. Ediz, D. Yaron, B.A. Armitage, J. Am. Chem. Soc. 129 (2007) 5710–5718.